

## RESEARCH ARTICLE

# Atmospheric pressure matrix-assisted laser desorption/ionization mass spectrometry of engine oil additive components

Lamprini Ramopoulou<sup>1,2</sup>  | Lukas Widder<sup>1</sup>  | Josef Brenner<sup>1</sup> |  
Andjelka Ristic<sup>1</sup>  | Günter Allmaier<sup>2</sup> 

<sup>1</sup>AC2T research GmbH, Wiener Neustadt, Austria

<sup>2</sup>Institute of Chemical Technologies and Analytics, TU Wien (Vienna University of Technology), Vienna, Austria

**Correspondence**

L. Ramopoulou, AC2T research GmbH, Viktor Kaplan-Straße 2/C, 2700 Wiener Neustadt, Austria.  
Email: lamprini.ramopoulou@ac2t.at

**Funding information**

Austrian COMET-Program, Grant/Award Number: 872176; TU Wien Bibliothek

**Rationale:** The efficiency of lubricants strongly depends on the content of functional additives. In order to assess the chemical and structural changes taking place in the lubricating oil and its additives during operation, it is essential to develop a method for simple and prompt analysis.

**Methods:** Two single additives as well as a fully formulated engine oil were analysed using an atmospheric pressure matrix-assisted laser desorption/ionization (AP-MALDI) source coupled to a linear trap quadrupole Orbitrap XL hybrid tandem mass spectrometer and compared with results obtained by means of electrospray ionization (ESI) including additional low-energy collision-induced dissociation (LE-CID). The identification of additives directly from technical surfaces was simulated by using steel substrates as AP-MALDI targets with varying roughness.

**Results:** After assessment and selection of the most suited AP-MALDI matrix it was found that pure additives such as calcium sulfonate and zinc dialkyldithiophosphates (ZDDPs) could well be identified with abundant signal intensity based on their elemental composition. Molecular identification was corroborated by LE-CID in ESI mode. Additionally, additives present in the fully formulated commercial oil such as ZDDPs and salicylates could be reliably identified based on the elemental composition of the deprotonated molecules by means of the Orbitrap unit on different substrates including steel surfaces with high roughness.

**Conclusions:** AP-MALDI is an efficient technique for determination of lubricant additives directly from commercial oil blends. Identification of additive components was also achieved on steel surfaces with high roughness as applied in tribological systems and thus it is expected that it will be possible to assess additive degradation in real applications, enabling more effective and timely maintenance measures.

This is an open access article under the terms of the Creative Commons Attribution-NonCommercial-NoDerivs License, which permits use and distribution in any medium, provided the original work is properly cited, the use is non-commercial and no modifications or adaptations are made.

© 2022 AC2T research GmbH. Rapid Communications in Mass Spectrometry on behalf of John Wiley & Sons Ltd.

## 1 | INTRODUCTION

Liquid lubricants consist of one or more base oils and up to around 25% v/v of functional additives. Their main tasks, among others, involve: improving the friction and wear performance between interacting surfaces; enabling the control of friction; serving as a coolant or heat transfer medium; increasing resistance against corrosion, oxidation and degradation by acids<sup>1,2</sup>; and to keep surfaces clean.<sup>3,4</sup>

There is a wide range of additives such as zinc dialkyldithiophosphates (ZDDPs), which are known for their anti-wear, anti-corrosion and anti-oxidant functionality. Therefore, ZDDPs are often applied in engine lubricants as well as hydraulic and transmission oils.<sup>5</sup> Other relevant additives include overbased calcium sulfonates and salicylates which are widely used as broad-spectrum detergents and anti-wear additives. In addition, calcium sulfonates are known for their rust-inhibiting and acid-binding properties. In particular, overbased detergents are used as additives in engine oils to prevent the development of varnish and other deposits on hot metal surfaces and to neutralize the acid products formed during combustion.<sup>6-9</sup>

During sliding, a thin tribofilm can form on the rubbing surfaces, and this can reduce friction and wear in numerous cases. The composition of these tribofilms has been extensively investigated by various measurement techniques, such as X-ray photoelectron spectroscopy (XPS),<sup>8,10-13</sup> X-ray absorption spectroscopy,<sup>14-16</sup> and transmission electron microscopy (TEM) combined with focused ion beam (FIB) cutting.<sup>17</sup> Other available techniques include X-ray absorption near edge structure (XANES),<sup>16,18</sup> RAMAN spectroscopy,<sup>19</sup> scanning electron microscopy (SEM) with energy-dispersive X-ray spectroscopy (EDS),<sup>8,20-22</sup> Fourier-transform infrared (FTIR) spectroscopy,<sup>23,24</sup> electrospray ionization mass spectrometry (ESI-MS),<sup>25,26</sup> high-field asymmetric waveform ion mobility spectrometry coupled with mass spectrometry (FAIMS-MS),<sup>27</sup> or dynamic time-of-flight secondary ion mass spectrometry (TOF-SIMS).<sup>28</sup>

Direct surface analysis techniques such as desorption electrospray ionization (DESI-MS)<sup>29</sup> oil analysis and direct analysis in real time coupled with mass spectrometry (DART-MS)<sup>30</sup> have been applied for quantitative analysis of a commercial lubricant antioxidant additive in a base oil, while mass spectrometric imaging (MSI) by means of laser desorption/ionization reflectron time-of-flight mass spectrometry (LDI-RTOF-MS) was used to analyse *ex situ* oil components applied as lubricant additives in a tribological layer of a tribologically stressed surface.<sup>31</sup> Another analytical technique employed for direct analysis of base oils and additives is the atmospheric solids analysis probe in conjunction with ion mobility mass spectrometry (ASAP-IM-MS).<sup>32,33</sup>

Atmospheric pressure matrix-assisted laser desorption/ionization (AP-MALDI) is complimentary to the previously mentioned analytical methods and already a powerful tool to analyse proteomes and lipidomes.<sup>34,35</sup> Moreover, this technique has also been already successfully adopted for characterization of lubricant oils to detect

additives such as anti-oxidants<sup>36</sup> and frictions modifiers<sup>37</sup> directly from base oil solutions as well as from tribologically stressed steel surfaces.<sup>38</sup> In addition, previous studies have used different surface materials as AP-MALDI targets, with the gold-coated steel target showing superior desorption/ionization yield.<sup>35,36,39</sup>

AP-MALDI is an efficient analytical method because the time-consuming and costly sample preparation necessary for other techniques is significantly reduced. Furthermore, for this method atmospheric pressure is present, thus avoiding excessive vaporization of volatile compounds. However, no comprehensive analysis has yet been carried out in a fully formulated engine oil by means of AP-MALDI, neither on gold-coated steel targets nor on other material surfaces of industrial interest, which would be a major step towards direct chemical analysis of tribofilms in wear tracks. In this study, a fully formulated SAE 0W-20 engine oil and two pure additives, calcium sulfonate and ZDDP, were analysed with AP-MALDI on gold-coated steel targets and on AISI 52100 steel discs, a typical bearing material, with different roughnesses.<sup>36</sup> The AP-MALDI target materials were varied to investigate differences in desorption/ionization abundances in order to simulate realistic surface conditions of industrial component samples.

## 2 | EXPERIMENTAL

### 2.1 | Chemicals and materials

In this study an engine oil and two separate additive components were used for AP-MALDI measurements. The engine oil was a commercially available fully formulated SAE 0W-20 engine oil with viscosity index 172 (dynamic viscosity 48 mm<sup>2</sup>/s (40°C) and 9 mm<sup>2</sup>/s (100°C)). A detailed overview and additional properties of the selected engine oil were provided by Besser et al.<sup>26</sup> The two additives, commercial zinc dialkyldithiophosphate (ZDDP, liquid, received pre-dissolved in diluent oil and used as received) and calcium sulfonate (55% v/v mixture in mineral oil), were purchased from LLK-Naftan (Vienna, Austria) and Rhein Chemie (Vienna, Austria), respectively. For AP-MALDI-MS experiments the following AP-MALDI matrices were applied: sinapic acid (SA, ≥99,0%), 2,5-dihydroxybenzoic acid (DHBA, ≥99,0% HPLC grade), α-cyano-4-hydroxycinnamic acid (CHCA, ultra-pure), purchased from Sigma-Aldrich (Vienna, Austria), as well as dithranol (DTH, ≥ 98,0%, for MALDI), purchased from Fisher Scientific (Vienna, Austria). LC/MS grade solvents chloroform (≥ 99,9%, HPLC gradient grade), purchased from Honeywell (Vienna, Austria), and methanol (≥ 99,9%, HPLC gradient grade), purchased from Sigma-Aldrich, were additionally used for sample preparation.

A standard AP-MALDI gold-coated steel target (hereafter referred to as “gold target”) was used as surface reference material provided by MassTech (Columbia, MD, USA). AISI 52100 steel discs (hereafter referred to as “steel disc”) with a diameter of 2.5 cm were chosen as complementary AP-MALDI target materials, in order to simulate realistic behavior on technical surfaces (e.g. in

triboexperiments) as well as to investigate the influence of surface roughness on additive desorption/ionization abundances. The steel sample targets were surface ground to varying roughness values using metallographic methods (see Figure 1). The average surface roughness  $R_a$  of the samples was measured using a Leica DCM 3D-confocal microscopy instrument (Leica Microsystems, Wetzlar, Germany). The resulting roughness values of applied target specimens are given in Figure 1.

## 2.2 | AP-MALDI-MS experiments

The AP-MALDI PDF+ ion source (MassTech, Columbia, MD, USA) on the LTQ Orbitrap XL hybrid tandem mass spectrometer was utilized for all AP-MALDI-MS experiments in the present study. All AP-MALDI-MS results were obtained with reduced mass resolution of  $m/\Delta m$  30,000 at FWHM (full width at half maximum) to reduce analysis time of molecules within the mass analyser and increase the number of scan events due to the limited volume of available sample compared with ESI experiments and with mass accuracy better than 7 ppm. This allowed detection of the protonated and deprotonated molecules with chemical structures already known from ESI measurements. Detailed experimental parameters and results of correlating ESI-MS measurements are given in the supporting information. The lubricant specimens were deposited on the surface of the selected AP-MALDI target and irradiated with UV laser light pulses of the solid-state Nd:YAG laser at a wavelength of 355 nm. The laser was operated in spiral motion mode (screened area  $\sim 2 \text{ mm}^2$ ) at a repetition rate of 10 Hz. The pulse width was at 3–5 ns (FWHM). In this study a pulse energy of 40  $\mu\text{J}$  was used and, to optimize the signal intensity, the pulsed dynamic focusing (PDF) was set to 25  $\mu\text{s}$ . For all AP-MALDI-MS experiments the automatic gain

control of the LTQ Orbitrap XL was turned off in order to achieve an equal number of laser shots for all single scan events.<sup>40,41</sup> The injection time was set to 500 ms and total acquisition time per scan was set to 0.5 min.<sup>38</sup> Operating conditions were applied according to tuning optimization of parameters: (a) for negative ion mode: AP-MALDI plate voltage,  $-2.6 \text{ kV}$ ; capillary temperature,  $200^\circ\text{C}$ ; capillary voltage,  $-15 \text{ V}$ ; tube lens voltage-120 V and (b) for positive ion mode: AP-MALDI plate voltage,  $3.5 \text{ kV}$ ; capillary temperature,  $275^\circ\text{C}$ ; capillary voltage,  $10 \text{ V}$ ; tube lens voltage 80 V.

The AP-MALDI matrices were each dissolved in a solution of 7:3 (v/v) chloroform/methanol at a concentration of 10 mg/mL. The pure additives and the engine oil were separately diluted in the same solvent to obtain a volume ratio of 1:10 (v/v). For all the AP-MALDI-MS measurements the ratio of sample to matrix<sup>38</sup> was 1:10 (v/v). Additional studies of the engine oil were performed at ratios of 1:30 and 1:50 (v/v) with DTH matrix only to assess whether the dilution factor of the matrix acts differently, e.g. increased ratio of analyte to matrix ions and signal-to-noise ratio. Droplets of 1.5  $\mu\text{L}$  of the resulting solutions were deposited on the different targets and let dry at room temperature resulting in spot areas of  $\sim 12.5 \text{ mm}^2$ . Before each AP-MALDI-MS experiment, the target surfaces were thoroughly cleaned using methanol.

## 2.3 | Microscopy analyses

Prior to and after AP-MALDI-MS measurements, optical microscopy was performed on the dried sample spots of fully formulated SAE 0W-20 engine oil with DTH matrix deposited on gold and steel targets, making use of a AXIO Imager M2m reflected light microscope (Carl Zeiss Microscopy, Jena, Germany) in bright field mode. Selected AP-MALDI spots from the above sample were analysed further with environmental scanning electron microscopy (ESEM) using a JSM IT300 microscope (JEOL, Tokyo, Japan) with an accelerating voltage of 15 kV in back-scattered electrons (BSE) mode. To avoid evaporation or decomposition and charging effects of the analysed compounds, they were analysed in low vacuum and the pressure during ESEM measurements was set to 50 Pa.

## 3 | RESULTS AND DISCUSSION

### 3.1 | Evaluation of peak abundances depending on matrix/analyte crystal structure and distribution

For AP-MALDI-MS measurements, the analyte/matrix solutions of fully formulated SAE 0W-20 engine oil and DTH matrix were spotted on the gold target. For all samples, it was obvious that the evaporation of chloroform and methanol occurred asynchronously, resulting in an inhomogeneous distribution of the matrix and thus inhomogeneous crystal formation, density and sizes (see Figure 2A). Hence, the signal response from areas with differently shaped matrix/analyte crystals was examined performing six AP-MALDI-MS scan

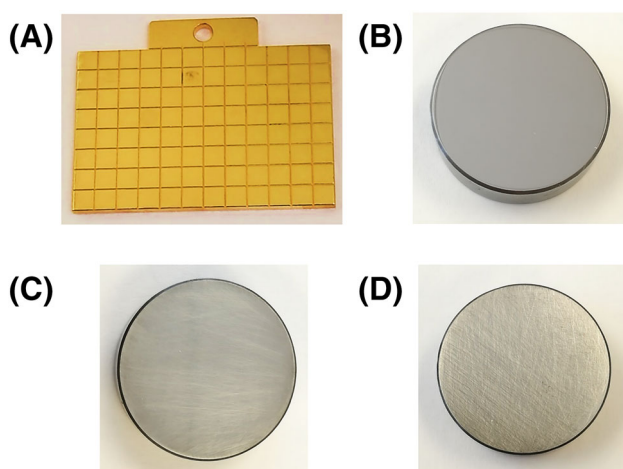


**FIGURE 1** Target specimens with varied surfaces roughness: (A), standard AP-MALDI Au-covered steel target (reference)  $R_a = 0.02 \mu\text{m}$ ; and AISI 52100 steel discs (B) mirror-polished,  $R_a < 0.01 \mu\text{m}$ ; (C) low roughness,  $R_a = 0.06 \mu\text{m}$ ; (D) high roughness,  $R_a = 0.130 \mu\text{m}$  [Color figure can be viewed at [wileyonlinelibrary.com](http://wileyonlinelibrary.com)]

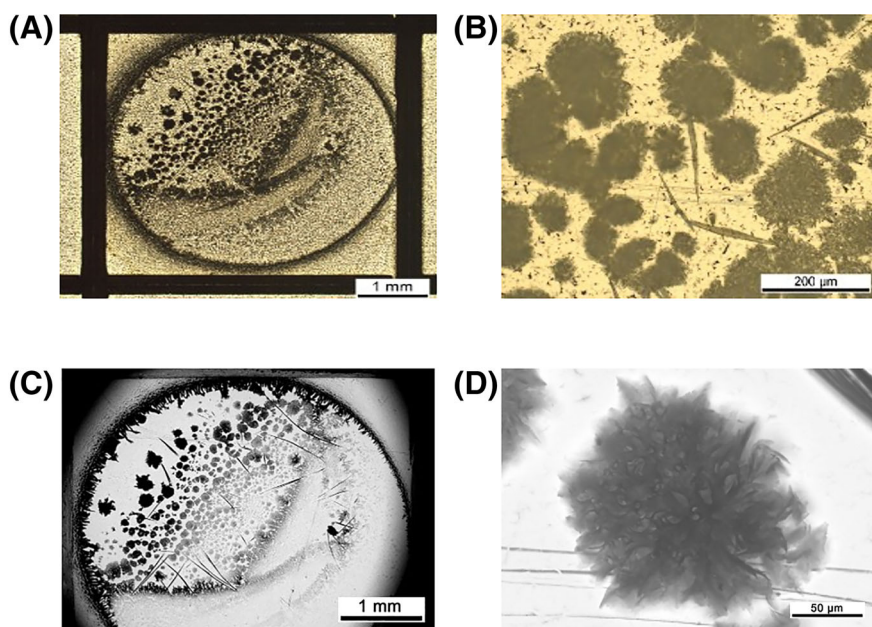


**FIGURE 2** Overview of a matrix/analyte solution spotted on a gold target (fully formulated SAE 0W-20 engine oil and DTH matrix): (A), light microscope overview and (B), detail as well as (C), ESEM overview and (D), enlarged detail [Color figure can be viewed at [wileyonlinelibrary.com](http://wileyonlinelibrary.com)]

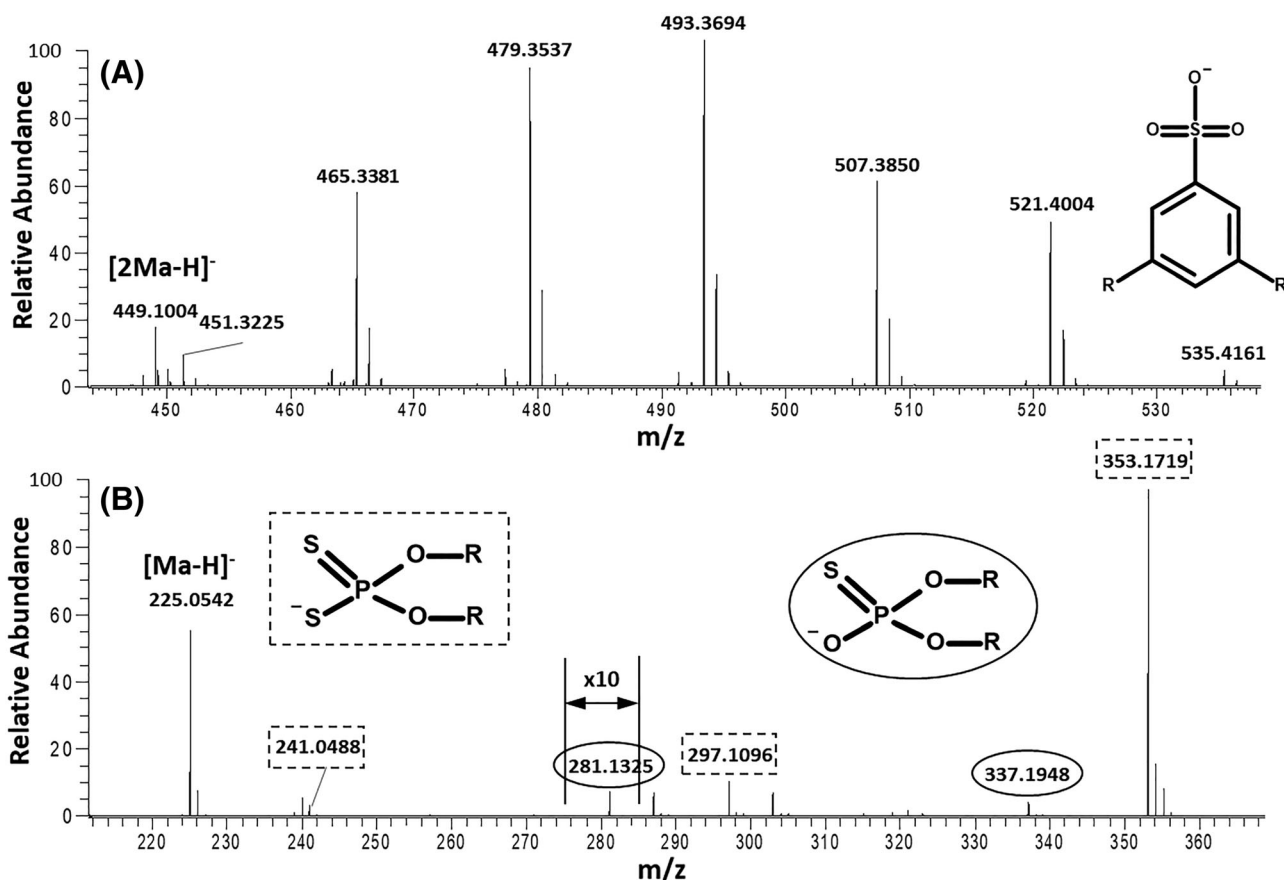


**FIGURE 3** AP-MALDI mass spectra in negative ion mode of pure additive samples with DTH matrix applied: (A), calcium sulfonates and (B), ZDDP (dashed line: dithiophosphates; solid line: O,O-phosphorothioates). For demonstration of the AP-MALDI mass spectra, results obtained with DTH matrix were selected due to most abundant signal response

events on each spot. The light microscopic images compared with the AP-MALDI-MS results indicate that measurements are to be performed at areas where the crystals were visibly larger (see Figure 2B), compared with other areas with denser but very small

crystals. Only at these positions could the desired peaks be detected with sufficient signal intensity. Comparable results were obtained on all investigated AP-MALDI target surfaces used for this study. Additionally, ESEM was applied (see Figure 2C) to compare crystal

manifestations and shapes. The larger crystal accumulations have been observed to form perpendicularly to the considered target surface and to form a pronounced 3D-contour (see Figure 2D).

### 3.2 | Identification of additive components from reference target

In this study, pure commercial ZDDP and calcium sulfonate in base oil were diluted separately to obtain concentrations of 1:10 (v/v) and

**TABLE 1** Maximum AP-MALDI-MS ion abundances of representative deprotonated molecules of calcium sulfonate ( $m/z$  493.3694) and dithiophosphate ( $m/z$  353.1719) in negative ion mode

Applied matrix component	Ca-sulfonate $m/z$ 493.3694	Dithiophosphate $m/z$ 353.1719
DTH	$3.7 \times 10^4$	$5.0 \times 10^4$
CHCA	$2.6 \times 10^3$	$3.7 \times 10^3$
2,5-DHBA	$1.0 \times 10^3$	$6.9 \times 10^2$
SA	$1.9 \times 10^3$	$3.4 \times 10^3$

were measured in negative ion AP-MALDI mode. Since the maximum ion abundances of the detected protonated and deprotonated molecule peaks with AP-MALDI-MS was  $10^4$  it was difficult to perform LE-CID fragmentation of the precursor ions. Therefore, to confirm the types of molecules of the additive components the elemental compositions obtained by means of AP-MALDI were correlated to ESI results. Four different matrices (DTH, CHCA, 2,5-DHBA and SA) were separately mixed with the above-mentioned pure additive components as well as the fully formulated engine oil in a sample/matrix ratio of 1:10 (v/v) and applied on a standard gold-coated steel AP-MALDI target for MS examinations in negative and positive ion mode.

In addition to the peaks observed in ESI-MS in negative ion mode, abundant peaks of matrix  $[Ma-H]^-$  (Ma, matrix molecule) and matrix cluster ions  $[2Ma-H]^-$  were detected as well.  $[Ma-H]^-$  and  $[2Ma-H]^-$  ions were observed for DTH at  $m/z$  225.0542 and 449.1004, for CHCA at  $m/z$  188.0343 and 377.0757, for 2,5-DHBA at  $m/z$  152.0108 and 307.0440, and for SA at  $m/z$  223.0597 and 447.1270, respectively. Moreover, matrix ions  $[Ma+H]^+$  and matrix cluster ions  $[2Ma+H]^+$  were also determined in AP-MALDI positive ion mode for matrix compounds DTH ( $m/z$  227.0708 and 451.1188),

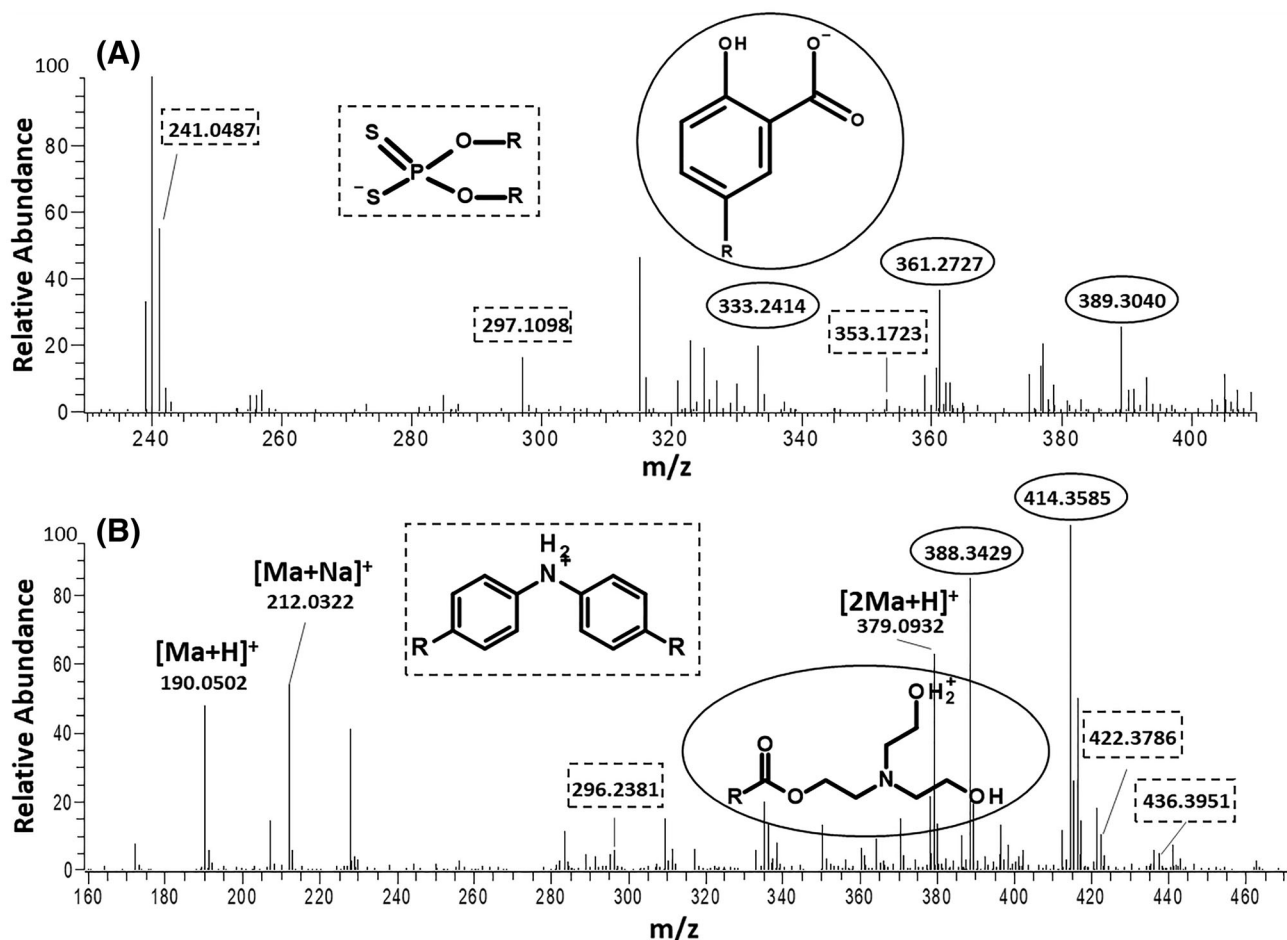


**FIGURE 4** Mass spectra obtained by AP-MALDI-MS of engine oil SAE 0W-20 obtained (A), in negative ion mode with DTH matrix applied (dashed line: dithiophosphates; solid line: salicylates) and (B), in positive ion mode with CHCA matrix applied (dashed line: diphenylamines; solid line: amine ethyl esters)



CHCA ( $m/z$  190.0502 and 379.0932), 2,5-DHBA ( $m/z$  155.0329), as well as SA ( $m/z$  225.0743 and 449.1416).

AP-MALDI-MS was applied in negative ion mode for calcium sulfonates. All deprotonated molecules of the calcium sulfonate additive found in ESI-MS were also detected in AP-MALDI-MS for all four applied matrix compounds. However, with DTH as matrix, ion abundances at least a factor of 10 higher were found for the desired deprotonated molecules. Measurements of the sulfonate ions detected by AP-MALDI at  $m/z$  451.3225 (C21), 465.3381 (C22), 479.3537 (C23), 493.3694 (C24), 507.3850 (C25), 521.4004 (C26), and 535.4161 (C27) yielded the same  $m/z$  values within the instrument accuracy compared with ESI results (see Figure 3A and supporting information).

For ZDDP, similar results were observed compared with calcium sulfonate, where the DTH matrix yielded higher ion abundances, too. The deprotonated ZDDP fragment ions dithiophosphates with  $m/z$  values of 241.0488 (C4-C4), 297.1096 (C4-C8), and 353.1719 (C8-C8) and the *O,O*-phosphorothioates with  $m/z$  281.1325 (C4-C8) and 337.1948 (C8-C8), observed already in ESI-MS measurements (see supporting information), were also detected with AP-MALDI (see Figure 3B).

The detected matrix ions and matrix cluster ions exceeded the abundances of the additive peaks. Using DTH matrix solution, for

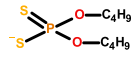
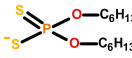
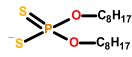
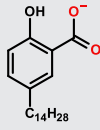
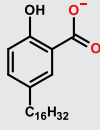
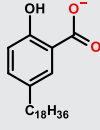
both additives the ion abundances of representative additive peaks were increased by a factor of 10 compared with the other matrices applied. The results were comparable for all detected additive peaks. Maximum ion abundances of representative peaks selected for both additives are given in Table 1. The total ion count (TIC) for ESI experiments exceeded AP-MALDI values and usually was in the range of  $10^7$  to  $10^8$  ions and, thus, at least  $10^3$  times higher. Measurements performed with AP-MALDI-MS could lead to complex mass spectra due to the presence of matrix peaks. However, the high resolving power of the Orbitrap mass analyser allowed the detection of additive peaks with known  $m/z$  values with the drawback of lower ion abundances in comparison with ESI-MS.

The calcium sulfonate additive sample was analysed in positive ion mode with AP-MALDI using all four matrices. However, due to very low ion abundances no additive or adduct peaks could be detected.

### 3.3 | Identification of commercial engine oil components from reference target

Further analyses were performed for the fully formulated SAE 0W-20 engine oil in negative and positive ion mode with all four matrices

**TABLE 2** Measured  $m/z$  values and chemical structures of components identified in the engine oil SAE 0W-20 obtained by means of ESI-MS and AP-MALDI-MS in negative ion mode including deviations of the measured  $m/z$  values

Name	Molecular formula	Chemical structure	Nominal value ( $m/z$ )	ESI ( $m/z$ )	$\Delta M/M$ (ppm)	AP-MALDI ( $m/z$ )	$\Delta M/M$ (ppm)
Dialkyl dithiophosphates	$C_8H_{18}O_2PS_2^-$		241.0491	241.0483	3.3	241.0487	1.7
	$C_{12}H_{26}O_2PS_2^-$		297.1117	297.1104	4.4	297.1098	6.4
	$C_{16}H_{34}O_2PS_2^-$		353.1743	353.1728	4.2	353.1723	5.7
Salicylates	$C_{21}H_{33}O_3^-$		333.2435	333.2421	4.2	333.2414	6.3
	$C_{23}H_{37}O_3^-$		361.2748	361.2733	4.2	361.2727	5.8
	$C_{25}H_{41}O_3^-$		389.3061	389.3045	4.1	389.3040	5.4

DTH, SA, CHCA and 2,5-DHBA. Analysis of the engine oil SAE OW-20 by means of AP-MALDI in negative ion mode with DTH matrix applied exhibited the additive ZDDP including the variety of alkyl chain lengths: dibutyl dithiophosphate ( $m/z$  241.0487), dihexyl dithiophosphate ( $m/z$  297.1098), dioctyl dithiophosphate ( $m/z$  353.1723), as well as the salicylate detergents ( $m/z$  333.2414 (C14);  $m/z$  361.2727 (C16);  $m/z$  389.3040 (C18)) (see Figure 4A). The  $m/z$  values and chemical structures of components identified are listed in Table 2. Similar to the previous analysis of the single additive components, the ion abundances of the investigated signals in the AP-MALDI-MS spectra were  $10^3$  to  $10^4$  times lower than the corresponding peaks detected by ESI-MS (cf. Table 3). The obtained AP-MALDI-MS results allowed determination of the elemental

composition and corresponded to the ions detected in ESI mode. Furthermore, it was observed in both methods (ESI and AP-MALDI) that ZDDP fragment ions of residual impurities with shorter alkyl chain length showed higher ion abundances.

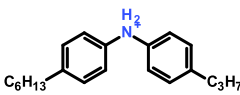
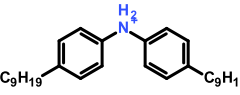
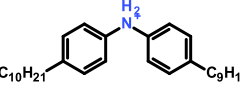
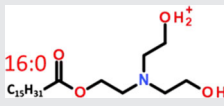
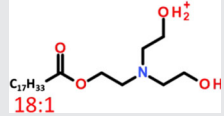
When SA matrix was applied, only the detergent (salicylate) molecules could be detected. Ion abundances were observed a factor of 10 lower, compared with the use of DTH matrix. The desired peaks were not detected with CHCA nor with 2,5-DHBA matrix. However, peaks of all matrices  $[Ma-H]^-$  and matrix cluster ions  $[2Ma-H]^-$  were observed. The sample/matrix ratio was set to 1:10 (v/v) for all AP-MALDI-MS measurements, as it was shown that for ratios 1:30 and 1:50 (v/v) with higher matrix concentrations, the molecular peaks investigated were suppressed and yielded lower signal intensities or could not be detected at all. For further investigations in the negative ion mode on steel targets, only DTH was used as matrix with the above-mentioned sample/matrix ratio.

Using AP-MALDI-MS in positive ion mode with CHCA and DTH as matrices for the engine oil the corresponding aminic anti-oxidants nonyldiphenylamine ( $m/z$  296.2381), dinonyldiphenylamine ( $m/z$  422.3786) and nonadecyldiphenylamine ( $m/z$  436.3951) as well as the fatty amine friction modifier 2-[bis(2-hydroxyethyl)amino] ethyl esters at  $m/z$  388.3429 (C16:0) and 414.3585 (C18:1) were detected. The obtained mass spectra of the additive ions are given in Figure 4B. The structures of found additive molecules are shown in Table 4. For both applied matrices the ion abundances of similar peaks had the same

**TABLE 3** Maximum AP-MALDI ion abundances of representative ZDDP ( $m/z$  241.0487) and salicylate ( $m/z$  361.2727) additive deprotonated molecules detected in SAE OW-20 samples in negative ion mode

Matrix component applied	ZDDP $m/z$ 241.0487	Salicylate $m/z$ 361.2727
DTH	$6.1 \times 10^3$	$3.6 \times 10^3$
CHCA	-	-
2,5-DHBA	$4.8 \times 10^1$	$3.5 \times 10^1$
SA	$1.1 \times 10^2$	$3.7 \times 10^2$

**TABLE 4** Measured  $m/z$  values of and chemical structures of components identified in the engine oil SAE OW-20 obtained by means of ESI-MS and AP-MALDI-MS in positive ion mode including deviations of the measured  $m/z$  values

Name	Molecular formula	Chemical structure	Nominal value ( $m/z$ )	ESI ( $m/z$ )	$\Delta M/M$ (ppm)	AP-MALDI ( $m/z$ )	$\Delta M/M$ (ppm)
Diphenylamines	$C_{21}H_{30}N^+$		296.2373	296.2367	2.0	296.2381	2.7
	$C_{30}H_{48}N^+$		422.3781	422.3772	2.1	422.3786	1.2
	$C_{31}H_{50}N^+$		436.3938	436.3929	2.1	436.3951	3.0
Aminic ethyl esters	$C_{22}H_{46}O_4N^+$		388.3421	388.3413	2.1	388.3429	2.1
	$C_{24}H_{48}O_4N^+$		414.3578	414.3571	1.7	414.3585	1.7

order of magnitude. As previously observed, compared with ESI experiments, the ion abundances of obtained peaks in the AP-MALDI mass spectra again were around  $10^3$  times lower. Ion abundances are given in Table 5.

In the case of the matrices SA and 2,5-DHBA, the AP-MALDI analysis of the engine oil did not enable the detection of the anti-oxidant and friction modifier additives. DTH and CHCA could be used for the analysis of the fully formulated commercial oil samples in AP-MALDI-MS in positive ion mode. The peak abundances of the ions corresponding to the CHCA matrix applied were lower and more suppressed compared with the DTH matrix peaks. In addition, the analyte ions seem to be better desorbed/ionized with CHCA as a higher ion abundance was observed. This facilitated the observation of the expected peaks of the oil additives and CHCA was used as the preferred matrix for this analysis.

### 3.4 | Identification of additive components from steel targets

AP-MALDI-MS measurements of the single ZDDP additive component were performed on the gold-coated steel target. The resulting mass spectra were used as a reference due to their good consistency with ESI results and the obtained high ion abundances. Subsequently, three steel AP-MALDI targets with different surface roughness (cf. Figure 1) were applied. In Figure 5A the abundances of the main ZDDP peaks of the AP-MALDI-MS measurement in negative ion mode on the four different target materials are given. Additional representative images of spots on all four surface modifications are given in the supporting information, including interpretations and comparisons with other AP-MALDI studies.

Similar AP-MALDI-MS measurements were performed for Ca-sulfonate additive components (see Figure 5B). In the diagrams, it can be seen that the abundances measured on steel targets were roughly 80% (ZDDP) and 90% (Ca-sulfonate) lower than the results obtained with the reference gold target. However, since the measured  $m/z$  values were retrieved by means of high accuracy Orbitrap mass detection, it could be assumed that identification of deprotonated additive molecules was successful for all considered surface conditions of the different steel targets. Furthermore, both additives were associated with higher ion abundances on the polished steel target than on both steel targets with higher surface roughness.

**TABLE 5** Main ion abundances of representative aminic anti-oxidant ( $m/z$  388.3429) and fatty amine friction modifier ( $m/z$  414.3585) protonated molecules detected in commercial engine oil SAE 0W-20 by means of AP-MALDI-MS in positive ion mode

Applied matrix component	Anti-oxidant $m/z$ 388.3429	Friction modifier $m/z$ 414.3585
DTH	$1.3 \times 10^4$	$1.8 \times 10^4$
CHCA	$6.2 \times 10^4$	$7.3 \times 10^4$

### 3.5 | Identification of engine oil components from steel targets

Following the AP-MALDI-MS analysis and successful identification of single additive components, subsequently, the fully formulated SAE 0W-20 lubricant was analysed. This analysis was carried out in negative ion mode with DTH as matrix in a similar way on all four different target samples. Similar to previous measurements of the single additive components, it could be observed that on the steel targets the abundance of the main peaks was significantly lower compared with measurements on the gold target. It was however hardly possible to distinguish between the different qualities of the steel target surfaces. The corresponding results can be seen in Figure 6. The ion abundances of the desired molecules on the gold target were at least a factor of 10 higher than the corresponding peaks on the steel targets. However, this analysis of the commercial engine oil shows that the additive components ZDDP and salicylates could be very well identified through AP-MALDI-MS with high-resolution detection also on steel target surfaces with higher roughness. This indicated a good applicability of this analytical method also under realistic industrial surface conditions (e.g. quality control laboratory).

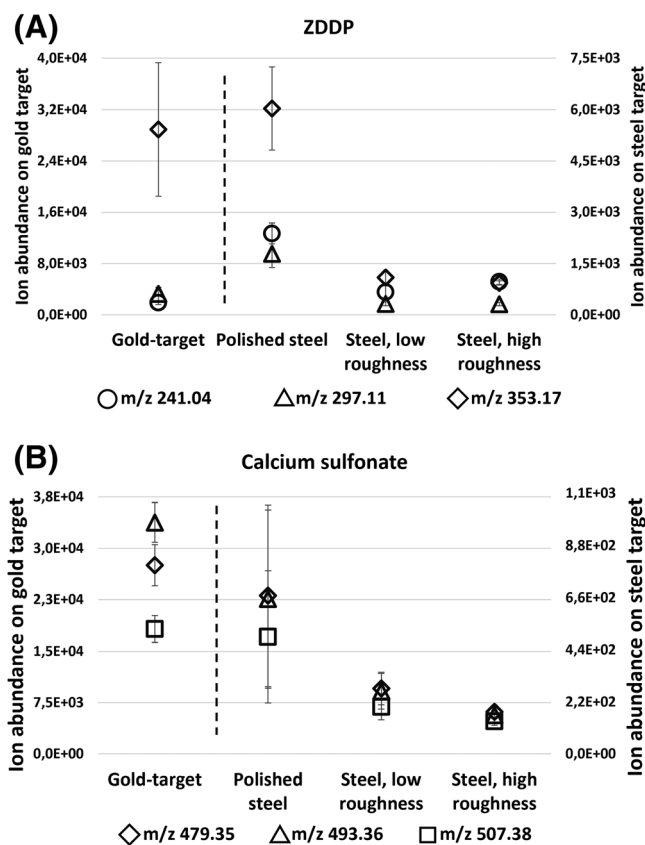


**FIGURE 5** Comparison of AP-MALDI-MS ion abundances obtained from various target surfaces in negative ion mode for (A), ZDDP and (B), Ca-sulfonate additives' deprotonated molecule peaks. The ion abundances obtained from the gold target are given on the left y-axis, whereas results from all other target surfaces are given on the right y-axis



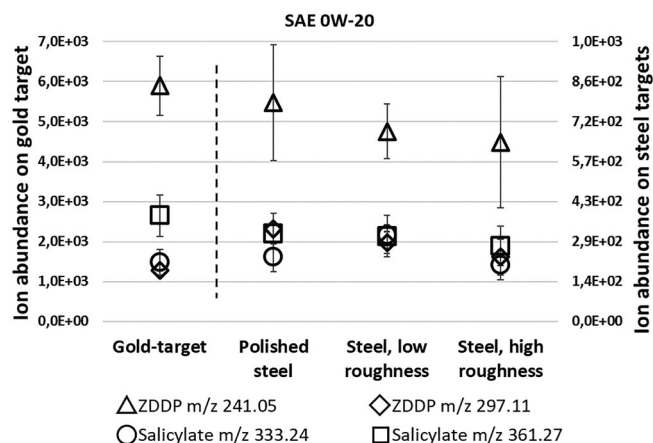


**FIGURE 6** Comparison of AP-MALDI-MS ion abundances of SAE 0W-20 additive components obtained from various target surfaces in negative ion mode. The ion abundances obtained from the gold target are given on the left y-axis, whereas results from all other target surfaces are given on the right y-axis (triangle, rhombus: ZDDP; circle, square: salicylate)

## 4 | CONCLUSIONS

In this study AP-MALDI ion generation coupled with an Orbitrap mass analyser was used to successfully perform a direct analysis of the calcium sulfonate and ZDDP additives as well as of fully formulated commercial SAE 0W-20 engine oil lubricant (containing ZDDP) in positive and negative ion mode. In order to confirm the detected chemical structures, the elemental compositions of the ions of interest were used combined with the results from ESI-MS and LE-CID-fragmentation technique, as provided in the supporting information.

AP-MALDI-MS experiments were performed on a gold target to evaluate the behavior and interactions of various matrix substances with the analyte ions. Results showed that DTH was the most suitable matrix for the assessment of the applied lubricant components in negative ion mode and CHCA for analysis in positive ion mode.

Additionally, the fully formulated SAE 0W-20 engine oil and the additives calcium sulfonate and ZDDP were analysed on steel discs with different surface roughness (as found in tribological experimental setups) by means of high-resolution and high-accuracy AP-MALDI-MS. All examined lubricant components could be detected and identified on the more technical surfaces very well, which demonstrates a good applicability of this technique also for realistic industrial surface conditions. However, it was found that increasing surface roughness of the target material resulted in a decrease in the measured peak abundance. In general, the measured peak abundance of all detected analyte ions on all steel targets was significantly lower compared with measurements on the reference AP-MALDI gold target.

Thus, it was shown that this method is very suitable for quick and reliable detection and identification of lubricant components directly from oil blends without the necessity for additional prior separation steps. In the so-called “soft” ionization process of AP-MALDI a substantially higher number of small molecules with varying polarity

becomes accessible for characterization compared with other methods such as ESI (e.g. due to the high number of background ions in the low  $m/z$  region, mainly molecules with high polarity are generated). Additional elucidation of tribological processes and characterization of degradation products and additive residues in used lubricants will be the subject of further investigations.

## ACKNOWLEDGMENTS

This work was funded by the “Austrian COMET-Program” (project InTribology, no. 872176) via the Austrian Research Promotion Agency (Österreichische Forschungsförderungsgesellschaft, FFG) and the federal states of Niederösterreich and Vorarlberg and has been carried out within the “Excellence Centre of Tribology” (AC2T research GmbH). The authors acknowledge TU Wien Bibliothek for financial support through its Open Access Funding Programme.

## PEER REVIEW

The peer review history for this article is available at <https://publons.com/publon/10.1002/rcm.9271>.

## DATA AVAILABILITY STATEMENT

Data available on request from the authors.

## ORCID

Lamprini Ramopoulou [ID https://orcid.org/0000-0002-4180-8458](https://orcid.org/0000-0002-4180-8458)

Lukas Widder [ID https://orcid.org/0000-0001-8297-8966](https://orcid.org/0000-0001-8297-8966)

Andjelka Ristic [ID https://orcid.org/0000-0001-6090-2776](https://orcid.org/0000-0001-6090-2776)

Günter Allmaier [ID https://orcid.org/0000-0002-1438-9462](https://orcid.org/0000-0002-1438-9462)

## REFERENCES

- Widder L, Grafl A, Lebel A, Tomastik C, Brenner J. Triboanalysis of hypoid gear components in drive trains. *Tribol und Schmierungstechnik*. 2011;58(2):11-15.
- Migdal CA. Lubricant Additives: Chemistry and Application. In: Rudnick LR, ed. 3rd ed. Boca Raton: CRC Press; 2017. doi:10.1201/9781315120621.
- Barnes AM, Bartle KD, Thibon VRA. A review of zinc dialkyldithiophosphates (ZDDPS): Characterisation and role in the lubricating oil. *Tribol Int*. 2001;34(6):389-395. doi:10.1016/S0301-679X(01)00028-7
- Shugarman AL. Lubricant base oils: Analysis and characterization of. In: *Encyclopedia of Analytical Chemistry*. Chichester: John Wiley & Sons, Ltd; 2006:1-9. doi:10.1002/9780470027318.a1825
- Dörr N, Brenner J, Ristić A, et al. Correlation between engine oil degradation, tribochemistry, and tribological behavior with focus on ZDDP deterioration. *Tribol Lett*. 2019;67(2):1-17. doi:10.1007/s11249-019-1176-5
- O'Connor SP, Crawford J, Cane C. Overbased lubricant detergents – A comparative study. *Lubr Sci*. 1994;6(4):297-325. doi:10.1002/lis.3010060402
- Cizaire L, Martin JM, Le Mogne T, Gresser E. Chemical analysis of overbased calcium sulfonate detergents by coupling XPS, ToF-SIMS, XANES, and EFTEM. *Colloids Surf A Physicochem Eng Asp*. 2004;238(1-3):151-158. doi:10.1016/j.colsurfa.2004.02.015
- Najman M, Kasrai M, Michael Bancroft G, Davidson R. Combination of ashless antiwear additives with metallic detergents: Interactions with neutral and overbased calcium sulfonates. *Tribol Int*. 2006;39(4):342-355. doi:10.1016/j.triboint.2005.02.014

9. Mang T, Bobzin K, Bartels T, Ikegami Y, Sato H, Matsuda N. *Industrial Tribology: Tribosystems, Friction, Wear and Surface Engineering, Lubrication*; 2010. doi:10.1002/9783527632572
10. De BarrosBouchet MI, Martin JM, Le-Mogne T, Vacher B. Boundary lubrication mechanisms of carbon coatings by MoDTC and ZDDP additives. *Tribol Int.* 2005;38(3):257-264. doi:10.1016/j.triboint.2004.08.009
11. Morina A, Neville A. Understanding the composition and low friction tribofilm formation/removal in boundary lubrication. *Tribol Int.* 2007; 40(10-12):1696-1704. doi:10.1016/j.triboint.2007.02.001
12. Parsaeian P, Ghanbarzadeh A, Van Eijk MCP, Nedelcu I, Neville A, Morina A. A new insight into the interfacial mechanisms of the tribofilm formed by zinc dialkyl dithiophosphate. *Appl Surf Sci.* 2017; 403:472-486. doi:10.1016/j.apsusc.2017.01.178
13. Zhang J, Ueda M, Campen S, Spikes H. Boundary friction of ZDDP tribofilms. *Tribol Lett.* 2021;69(8):1-17. doi: 10.1007/s11249-020-01389-4
14. Kim BH, Jiang JC, Aswath PB. Mechanism of wear at extreme load and boundary conditions with ashless anti-wear additives: Analysis of wear surfaces and wear debris. *Wear.* 2011;270(3-4):181-194. doi: 10.1016/j.wear.2010.10.058
15. Sharma V, Doerr N, Erdemir A, Aswath PB. Interaction of phosphonium ionic liquids with borate esters at tribological interfaces. *RSC Adv.* 2016;6(58):53148-53161. doi: 10.1039/c6ra11822d
16. Sharma V, Dörr N, Erdemir A, Aswath PB. Antiwear properties of binary ashless blend of phosphonium ionic liquids and borate esters in partially formulated oil (no Zn). *Tribol Lett.* 2019;67(42): doi: 10.1007/s11249-019-1152-0
17. Dawczyk J, Ware E, Ardakani M, Russo J, Spikes H. Use of FIB to study ZDDP tribofilms. *Tribol Lett.* 2018;66(155): doi: 10.1007/s11249-018-1114-y
18. Hsu CJ, Barrirero J, Merz R, et al. Revealing the interface nature of ZDDP tribofilm by X-ray photoelectron spectroscopy and atom probe tomography. *Ind Lubr Tribol.* 2020;72(7):923-930. doi:10.1108/ILT-01-2020-0035
19. Miklozic KT, Graham J, Spikes H. Chemical and physical analysis of reaction films formed by molybdenum dialkyl-dithiocarbamate friction modifier additive using Raman and atomic force microscopy. *Tribol Lett.* 2001;11:71-81. doi:10.1023/A:1016655316322
20. Gabler C, Tomastik C, Brenner J, Pisarova L, Doerr N, Allmaier G. Corrosion properties of ammonium based ionic liquids evaluated by SEM-EDX, XPS and ICP-OES. *Green Chem.* 2011;13(10):2869-2877. doi:10.1039/c1gc15148g
21. Nyberg E, Mouzon J, Grahm M, Minami I. Formation of boundary film from ionic liquids enhanced by additives. *Appl Sci.* 2017;7(5): doi: 10.3390/app7050433
22. Torres H, Caykara T, Rojacz H, Prakash B, Rodríguez RM. The tribology of Ag/MoS<sub>2</sub>-based self-lubricating laser claddings for high temperature forming of aluminium alloys. *Wear.* 2020;442-443: 203110. doi:10.1016/j.wear.2019.203110
23. Besser C, Dörr N, Novotny-Farkas F, Varmuza K, Allmaier G. Comparison of engine oil degradation observed in laboratory alteration and in the engine by chemometric data evaluation. *Tribol Int.* 2013;65:37-47. doi:10.1016/j.triboint.2013.01.006
24. Sejkorová M, Hurtová I, Jilek P, Novák M, Voltr O. Study of the effect of physicochemical degradation and contamination of motor oils on their lubricity. *Coatings.* 2021;11(1):1-18. doi: 10.3390/coatings11010060
25. Kassler A, Pittenauer E, Doerr N, Allmaier G. Development of an accelerated artificial ageing method for the characterization of degradation products of antioxidants in lubricants by mass spectrometry. *Eur J Mass Spectrom.* 2019;25(3):300-323. doi: 10.1177/1469066718811714
26. Besser C, Agocs A, Ronai B, et al. Generation of engine oils with defined degree of degradation by means of a large scale artificial alteration method. *Tribol Int.* 2019;132:39-49. doi:10.1016/j.triboint.2018.12.003
27. Da Costa C, Turner M, Reynolds JC, Whitmarsh S, Lynch T, Creaser CS. Direct analysis of oil additives by high-field asymmetric waveform ion mobility spectrometry-mass spectrometry combined with electrospray ionization and desorption electrospray ionization. *Anal Chem.* 2016;88(4):2453-2458. doi:10.1021/acs.analchem.5b04595
28. Cyriac F, Yi TX, Poornachary SK, Chow PS. Effect of temperature on tribological performance of organic friction modifier and anti-wear additive: Insights from friction, surface (ToF-SIMS and EDX) and wear analysis. *Tribol Int.* 2021;157:106896. doi:10.1016/j.triboint.2021.106896
29. Da Costa C, Reynolds JC, Whitmarsh S, Lynch T, Creaser CS. The quantitative surface analysis of an antioxidant additive in a lubricant oil matrix by desorption electrospray ionization mass spectrometry. *Rapid Commun Mass Spectrom.* 2013;27(21):2420-2424. doi: 10.1002/rcm.6690
30. Da Costa C, Whitmarsh S, Lynch T, Creaser CS. The qualitative and quantitative analysis of lubricant oil additives by direct analysis in real time-mass spectrometry. *Int J Mass Spectrom.* 2016;405:24-31. doi: 10.1016/j.ijms.2016.05.011
31. Gabler C, Pittenauer E, Dörr N, Allmaier G. Imaging of a tribolayer formed from ionic liquids by laser desorption/ionization-reflectron time-of-flight mass spectrometry. *Anal Chem.* 2012;84(24):10708-10714. doi:10.1021/ac302503a
32. Barrère C, Hubert-Roux M, Afonso C, Racaud A. Rapid analysis of lubricants by atmospheric solid analysis probe-ion mobility mass spectrometry. *J Mass Spectrom.* 2014;49(8):709-715. doi: 10.1002/jms.3404
33. Snyder SR, Wesdemiotis C. Elucidation of low molecular weight polymers in vehicular engine deposits by multidimensional mass spectrometry. *Energy Fuel.* 2021;35(2):1691-1700. doi:10.1021/acs.energyfuels.0c02702
34. Pittenauer E, Zehl M, Belgacem O, Raptakis E, Mistrik R, Allmaier G. Comparison of CID spectra of singly charged polypeptide antibiotic precursor ions obtained by positive-ion vacuum MALDI IT/RTOF and TOF/RTOF, AP-MALDI-IT and ESI-IT mass spectrometry. *J Mass Spectrom.* 2006;41(4):421-447. doi:10.1002/jms.1032
35. Pittenauer E, Kassler A, Haubner R, Allmaier G. Different target surfaces for the analysis of peptides, peptide mixtures and peptide mass fingerprints by AP-MALDI ion trap-mass spectrometry. *J Proteomics.* 2011;74(7):975-981. doi:10.1016/j.jprot.2010.10.003
36. Kassler A, Pittenauer E, Doerr N, Allmaier G. Electrospray ionization and atmospheric pressure matrix-assisted laser desorption/ionization mass spectrometry of antioxidants applied in lubricants. *Rapid Commun Mass Spectrom.* 2009;23(24):3917-3927. doi: 10.1002/rcm.4326
37. Widder L, Brenner J, Hutter H. Atmospheric pressure matrix-assisted laser desorption/ionization mass spectrometry of friction modifier additives analyzed directly from base oil solutions. *Eur J Mass Spectrom.* 2014;20(4):299-305. doi:10.1255/ejms.1283
38. Widder L, Ristic A, Brenner F, Brenner J, Hutter H. Modified-atmospheric pressure-matrix assisted laser desorption/ionization identification of friction modifier additives oleamide and ethoxylated tallow amines on varied metal target materials and tribologically stressed steel surfaces. *Anal Chem.* 2015;87(22):11375-11382. doi: 10.1021/acs.analchem.5b02793
39. Widder L. A novel approach to characterization of industrial lubricant additives in boundary surface tribofilms by atmospheric pressure matrix assisted laser desorption/ionization PhD Thesis. TU Wien; 2019:1-131.

40. Laiko VV, Moyer SC, Cotter RJ. Atmospheric pressure MALDI/ion trap mass spectrometry. *Anal Chem.* 2000;72(21):5239-5243. doi:10.1021/ac000530d
41. Garrett TJ, Prieto-Conaway MC, Kovtoun V, et al. Imaging of small molecules in tissue sections with a new intermediate-pressure MALDI linear ion trap mass spectrometer. *Int J Mass Spectrom.* 2007;260(2-3):166-176. doi:10.1016/j.ijms.2006.09.019

**How to cite this article:** Ramopoulou L, Widder L, Brenner J, Ristic A, Allmaier G. Atmospheric pressure matrix-assisted laser desorption/ionization mass spectrometry of engine oil additive components. *Rapid Commun Mass Spectrom.* 2022;36(9):e9271. doi:10.1002/rcm.9271

#### SUPPORTING INFORMATION

Additional supporting information may be found in the online version of the article at the publisher's website.